Contribution from the Research Staff,
Ford Motor Company, Dearborn, Michigan 48121

Crystal Structure of KCP(Br) [$K_2Pt(CN)_4Br_{0.30}\cdot 3.2H_2O$] as Determined by 300-K X-Ray and 8-K Neutron Diffraction Investigations

C. PETERS* and C. F. EAGEN

Received August 29, 1975 AIC50641X

As a result of detailed room-temperature x-ray diffraction, liquid helium temperature neutron diffraction, and thermal gravimetric studies, we have identified a third water molecule in the *P4mm* tetragonal unit cell of KCP(Br). The full complement of waters of hydration is 3.2, and, thus, the correct chemical formula is $K_2Pt(CN)_4Br_{0.30}\cdot 3.2H_2O$. Structurally, the additional water occupies those unit cells where the Br^- ion is absent, and, therefore, it should be termed a disordered "defect water"; it clearly contributes to the stability of the crystal. The structure is characterized by nearly planar, square $Pt(CN)_4^{1.7-}$ groups arranged in linear, polymeric chains parallel to the *c* axis with two slightly different Pt–Pt distances at 300 K. Each $Pt(CN)_4^{1.7-}$ unit is rotated 45° with respect to its nearest neighbors resulting in an arrangement of cubic antiprismatic, face-sharing polyhedra. These chains are supported and screened by a loosely bound, cubic antiprismatic structure of K^+, Br^-, and H_2O molecules. The crystal data for KCP(Br) are as follows: tetragonal system; Laue group *mmm*; space group No. 99, *P4mm*; x-ray (296 K), a = 9.890 (7) Å, c = 5.789 (3) Å; neutron (8 K), a = 9.829 (4) Å, c = 5.705 (3) Å, Z = 2. The diffractometric, θ–2θ scan, data refined to $R(F)$ values of 0.021 (x ray) and 0.039 (neutron).

I. Introduction

The mixed-valence Pt compounds $K_2Pt(CN)_4X_{0.3}\cdot nH_2O$, KCP(X), with X = Cl or Br and n = 3 are one-dimensional conductors of electricity at room temperature and exhibit broad metal–insulator transitions around 130 K. The discovery by Comès et al.[1] of diffuse planes of scattering perpendicular to the conducting tetragonal axis in a room-temperature x-ray diffraction study and the condensation of these planes into a reasonably sharp superlattice[2] at low temperatures[3,4] has generated considerable interest in the crystal structure and its relation to the one-dimensional electrical properties of this salt.

The x-ray work of Krogmann and Hausen[5] showed that the structure of KCP(Br) is characterized by widely separated linear chains of Pt atoms with intrachain Pt–Pt distances only slightly greater than those found in Pt metal. Thus, one is led to the picture of a one-dimensional electron band formed from the overlapping $5d_{z^2}$ orbitals of the Pt atoms. Since the Br^- ions accept an average of 0.60 electron per unit cell from the otherwise full Ptd_{z^2} band, one would expect KCP(Br) to be a conductor; however, one-dimensional systems are particularly susceptible to charge density wave (CDW) instabilities[6,7] which introduce energy gaps at the Fermi level. The existence of such a gap would give rise to electrical properties reminiscent of semiconductors and a corresponding sinusoidal lattice displacement wave characterized by the wave vector which spans the Fermi surface.

Recent neutron studies[8,9] have shown that the superstructure reflections can be adequately explained in terms of a rigid sinusoidal displacement of the nearly planar $Pt(CN)_4^{1.7-}$ anions in response to such a CDW instability. At low temperatures, the waves in neighboring chains tend to lock 180° out of phase. As the temperature is elevated, the phase coherence of the displacements on neighboring chains is gradually lost and the scattering spreads out onto a plane.

During the neutron investigation[9] of the response of the atoms in the unit cell to the CDW it was revealed that certain odd l reflections of the parent structure were not adequately described by the structure proposed by Krogmann and Hausen and we initiated room-temperature x-ray and, subsequently, 8-K neutron structure determinations.[10] Concurrent with our work other room and liquid nitrogen temperature x-ray and neutron structure determinations have been published.[11–15] All suffice to remedy the erroneous choice of centrosymmetric space group made in the earlier study, and all concur on the placement of the $Pt(CN)_4^{1.7-}$ anions, cations, and ~3.0 waters of hydration. However, there is a disparity among the results and with ours concerning either the number of Br^- sites and its stoichiometry and/or the full component of waters of hydration, their locations, and their orientations.

In this paper we present room-temperature x-ray diffraction, liquid helium temperature neutron diffraction, and thermal gravimetric studies which identify a third type of water molecule in the tetragonal unit cell of KCP(Br). The additional 0.2 mol of water fills the voids in the center of those unit cells where the Br^- ion is absent. Thus, it should be termed a disordered "defect water"; it clearly contributes to the stability of the crystal. (See Figure 1 for structure diagrams.)

II. Experimental Section

X-Ray Data. Single crystals of KCP(Br) were grown using the method developed by Saillant.[16] This procedure takes great care to prevent contamination of the crystals with Cl^- and OH^- ions. A sample of dimensions 0.12 × 0.12 × 0.20 mm was cleaved from an optically fault-free crystal, previously stored in the growth solution, and sealed in a glass capillary while working over damp filter paper to minimize water loss. Crystal quality, unit cell, and space group possibilities were determined from precession photographs. Lattice parameters were obtained from a least-squares refinement of 15 reflections centered with Mo Kα radiation, λ 0.71069 Å, on a Syntex $P2_1$ computer-controlled diffractometer.

Intensity data were collected using graphite-monochromated Mo Kα radiation at a takeoff angle of 4°. We employed 2.0° minimum θ–2θ scans allowing for spectral dispersion and variable scanning rates from 1 to 29°/min based on preliminary, stationary 2-s counts at the peak maximum. Stationary-background counts were taken at both ends of the scanning range maintaining a time ratio of 0.5 for the total background count vs. the reflection count.

A total of 1662 reflections were measured in the octant (hkl) to a limiting 2θ angle of 75°. After every 100 reflections the intensities of three standard reflections were measured as a check on electronic and crystal stability. A linear decrease of 9% in intensity from beginning to end of the experiment was observed in the ($h00$) and ($0k0$) standards while the ($00l$) standard remained constant. This pattern indicated a small rotational movement of the crystal about the needle axis. We corrected for this small effect using the drift factor

$$D = 1 + CN \sin \phi(\bar{d}, \bar{c})$$

where $\phi(\bar{d},\bar{c})$ is the angle between the diffraction vector, $\bar{d}$, and the needle axis, $\bar{c}$, of the crystal. The slope, C, was determined by a least-squares fit using the normalized intensity ratios of the two pertinent standard reflections and N, the sequence number of the observation.

The experiment resulted in a total of 686 independent reflections with $\Delta I/I < 0.5$ where ΔI is the statistical error in the measured

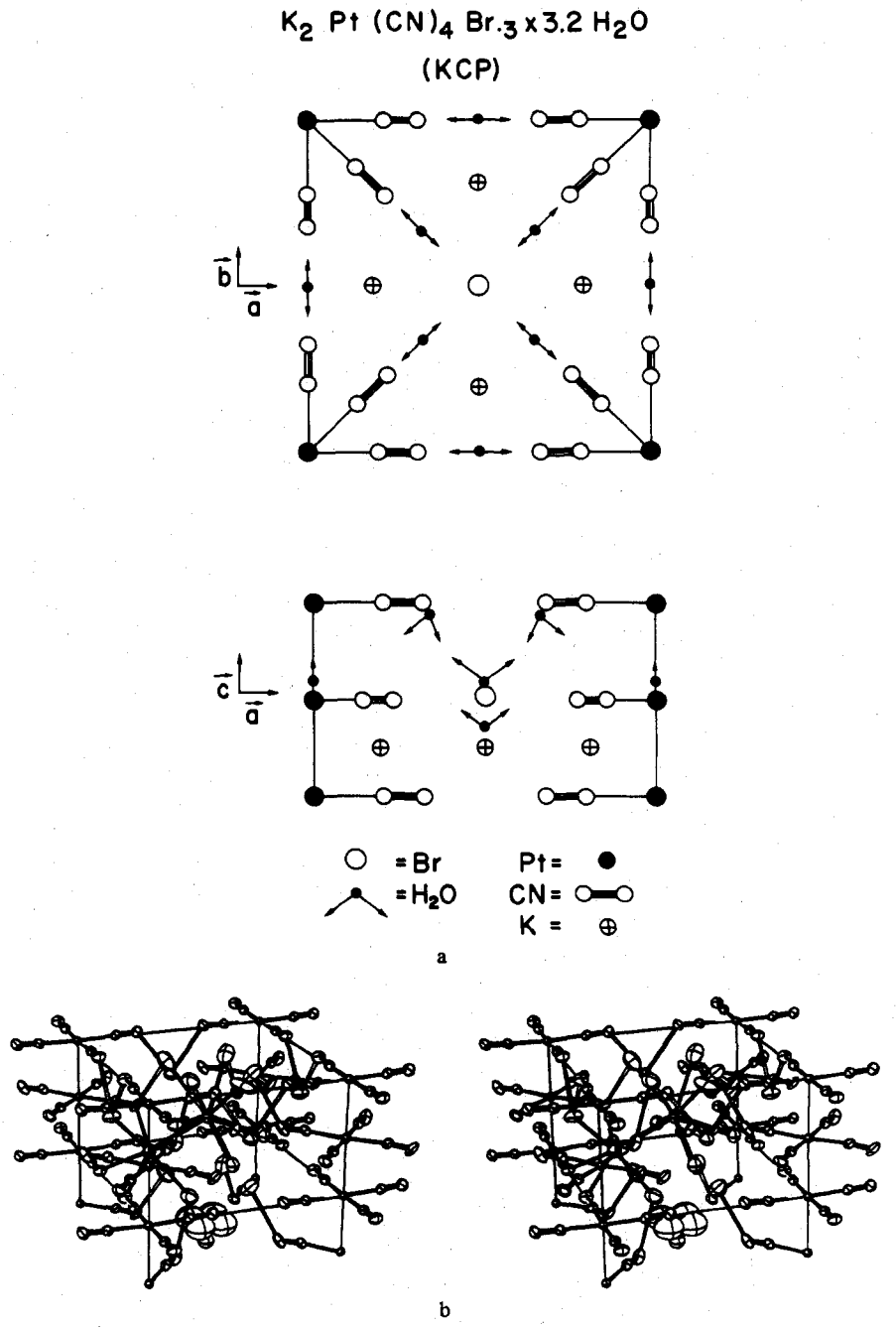

Figure 1. (a) Projection views along [001] and [010] directions and (b) stereoview[17e] of KCP(Br) showing defect Br ion in the upper cell and the defect water in the lower. Coordination of the K^+ and Br^- ions is shown using solid bonds; that of pure hydrogen bonds is shown using open bonds. The 50% probability thermal ellipsoids use neutron parameters for protons and x-ray parameters for the remainder of the atoms. Only the essential protons are drawn for the sake of clarity.

intensity, I. Standard procedures were used to correct for Lorentz–polarization[17a] and absorption effects.

The absorption factors[17b] varied from 2.0 to 3.3 and resulted in a 30% improvement in the agreement of 378 mirror related reflections, $I(hkl) = I(khl)$. Of the 686 independent reflections, the reflections measured in two asymmetric units had 2θ angles <50° and the additional 308 were collected in the reciprocal shell of radius 0.59 $< (\sin\theta)/\lambda \leq 0.8$ Å^{-1}.

Neutron Data. A cubic sample roughly 5 mm on edge, identical in preparation with the one used in the x-ray study, was cut from a larger crystal and sealed in an aluminum capsule. Since our spectrometer only allows for rotations about a vertical axis perpendicular to the 1.085-Å ^{239}Pu filtered neutron beam, the crystal was rotated about a crystallographic axis and the detector elevated in order to measure the reflections out of the equatorial plane. In this experimental configuration the rocking curve widths are strongly dependent on the detector elevation and diffraction angle. This necessitated changing the type of scan and detector collimation employed for reflections in different regions of reciprocal space to ensure that all of the scattered neutrons were accepted. The measured intensities were put on an "absolute" scale by normalizing to a fixed monitor count of the incident beam.

In order to measure most of the reflections inside the sphere defined by $(\sin\theta)/\lambda < 0.7$ Å^{-1}, part of the data were taken by rotating about the c axis and part by rotating about an a axis. Each data subset was separately corrected for absorption using the experimentally determined absorption coefficient, $\mu = 1.096$ cm^{-1}, and separate scale factors were employed in the refinement. The close agreement for the refined values of the two scale factors (within 1%) and the agreement of the 180 common reflections measured in both sample orientations attest to the validity of this procedure and show that the data do not suffer appreciably from systematic errors such as multiple Bragg scattering. Equivalent reflections for many of the larger reflections were measured and showed that errors arising from disparity

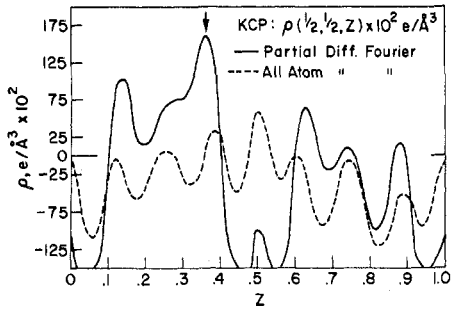

Figure 2. Difference Fourier line ($^1/_2$, $^1/_2$, z) from x-ray data. Note the defect site II peak at ($^1/_2$, $^1/_2$, 0.36) as well as noise peaks due to phase angle errors in the partial difference result (solid line). Dashed line shows result after site II peak is included in the structural model for KCP and identified as an oxygen atom.

in the incident neutron beam were minimal. Of the resulting 487 independent reflections, 440 satisfied the cutoff criterion of $\Delta I/I <$ 0.33.

III. Refinement

X-Ray Data. The Krogmann and Hausen structure refinement of KCP(Br),[5] using the space group No. 123, *P4/mmm*, assumes a mirror plane perpendicular to the c axis of the unit cell at $z = {}^1/_2$. This mirror plane necessitates an occupational disorder of four K^+ ions per unit cell among eight sites: four in the plane (x, y, $^1/_4$) and four others in the mirror-related plane (x, y, $^3/_4$). Also, this choice of space group required that the z coordinates of all the atoms be fixed by symmetry.

Based on this model, calculated structure factors for some of the (00l), $l = n + 1$, orders did not yield order of magnitude agreement with those observed by neutron diffraction. We found that much of this discrepancy could be mollified if we placed the four K^+ ions in fully occupied sites in one of the two planes and left the other plane vacant. This observation immediately led to the insight that the mirror plane perpendicular to the c axis was nonexistent in the real structure and, therefore, the noncentrosymmetric space group No. 99, *P4mm*, was the proper choice for the refinement of the KCP(Br) structure.

Starting with the four K^+ ions at $z = 0.25$, the 0.60 Br at the center of the cell, site I, and Krogmann's coordinates for the rest of the atoms, a least-squares refinement[17d] converged to a value of $R = 0.03 = \sum||F_o| - |F_c||/\sum|F_o|$ using isotropic thermal parameters. A subsequent Fourier difference map,[17c] Figure 2, indicated the existence of an additional atomic site at ($^1/_2$, $^1/_2$, 0.364), site II. Since the halide content of KCP is instrumental in determining the period of the CDW and is of some dispute,[18] site II was initially refined as a Br^- ion. Introducing anisotropic thermal parameters, as well as occupancy parameters for site I and site II, additional cycles of least squares refined to $R = 0.022$ and $R_w = \sum w(F_o - F_c)^2/\sum wF_o^2 = 0.026$. The weights, w, for the individual structure factors were assigned using the expression $w = 1/(\sigma)^2$ where $\sigma' = [\sigma^2 + (0.02F_o)^2]^{1/2}$ and σ is the statistical error in F_o. Some convergence problems during the refinement, caused by strong correlations among the occupancy and thermal parameters of the defect sites, were circumvented by using fractional parameter shifts and fixing the z coordinate for site II at 0.364.

While the R values indicated excellent agreement of the model with reality, the total occupancy of the defect sites, 8(0.076 + 0.013) = 0.71, was 18% larger than the 0.600 (6) value found by chemical analysis.[20] In addition, the magnitudes of the anisotropic thermal parameters, β_{ij}, for the site II Br^- compared to those for site I (see Table I) were disturbingly high because site II is nearer the four K^+ ions than is site I. In fact, the β_{ij} values for site II are the largest of all the scatterers in the unit cell, even larger than those for oxygen atoms in loosely bound water molecules. A Br^- identification for site II is further suspect because the distance from site II to a K^+ site of 3.09 Å is significantly shorter than the sum of the K^+ and Br^- ideal ionic radii, 3.26 Å.

Hence, we concluded that site II was not a Br^- scatterer but most likely contained fewer electrons, namely, an oxygen atom of an unsuspected water of hydration. Further cycles of least squares, while not significantly improving the discrepancy factors, did remove the thermal parameter anomaly, define the stoichiometry of the fully hydrated structure, and explain the nature of the site I–II defect structure in a logical manner.

Table I. Comparison of Occupancy and Anisotropic Thermal Parameters, U_{ij} (Å^2), for the Defect Site II ($^1/_2$, $^1/_2$, ~0.36), Depending on Identification as a Br Ion or Oxygen Atom, with Other Br and Oxygen Site Parameters (X-Ray Data Only)

Atom	Occupancy/unit cell	U_{11}	U_{22}	U_{33}
Site II, Br	0.104 (16)	0.1085 (451)	U_{11}	0.0964 (447)
Site II, O(3)	0.440 (32)	0.0659 (362)	U_{11}	0.0528 (265)
Site I, Br(1)	0.608 (8)	0.0273 (15)	U_{11}	0.0433 (19)
O(1)	4	0.0763 (74)	U_{11}	0.0778 (98)
O(2)	2	0.0421 (59)	0.0892 (99)	0.0317 (58)

Identification of site II as an O atom yields the refined occupational probabilities $n(Br^-) = 0.604$ (8) and $n(O) = 0.44$ (3) with $n(Br^-) + n(O) = 1.04$ (3). Since the two defect sites are only 0.9 Å apart, this result means that one or the other—but not both—of the two sites is always occupied in every unit cell. If a Br^- ion is absent, a water molecule fills the void and maintains the linearity of the $Pt(CN)_4^{1.7-}$ chains which would probably "kink" if the voids were not filled.

Refinement of the occupation probabilities of the oxygen atoms, O(1) and O(2), of the two other water molecules yielded values of 1.028 ± 0.028 and 1.11 ± 0.04, respectively, showing no loss of water from the x-ray specimen crystal. The occupation of these two sites was fixed at unity for the final cycles of refinement.

The final discrepancy factors are summarized as follows: $R = 0.021$ and $R_w = 0.026$ for all hkl; $R = 0.019$ and $R_w = 0.022$ for $l = 2n$; $R = 0.053$ and $R_w = 0.048$ for $l = 2n + 1$. The goodness of fit index, $[\sum w(F_o^2 - F_c^2)/(m - n)]^{1/2}$, was 1.04 for an $n = 54$ parameter model using $m = 686$ observations. For comparison, Krogmann reported values of $R = 0.073$, all hkl, and $R = 0.49$, $l = 2n + 1$, for KCP(Br). When we refined the published film data in the proper space group, *P4mm*, $R = 0.051$, all hkl, and R for the $l = 2n + 1$ orders decreased to 0.16.

The final structural parameters for KCP(Br) are shown in Tables II and III. These parameters resulted from a convergent refinement where all of the parameters but the occupation numbers for the two defect sites were varied using least-squares shifts of $0.2\Delta_i$. The form factors used were those for K^+, O^-, Br^-, C, N, and Pt, and the anomalous dispersion correction was applied to the Pt, Br^-, and K^+ form factors.[19]

Neutron Data. Although x-ray diffraction is sufficiently sensitive to locate the oxygen atom of the defect water molecule, it cannot see the associated hydrogen atoms in the presence of the strongly scattering Br^- ion and $Pt(CN)_4^{1.7-}$ complexes. This problem is not as severe in neutron diffraction because the coherent neutron scattering cross sections are more nearly uniform across the periodic table. In particular, the coherent scattering lengths for the elements Pt, O, and H are 0.95, 0.58, and −0.37, respectively. Since the defect water molecule is in a position which does not allow for strong hydrogen bonding, one would expect a large thermal disorder of the H atoms at elevated temperatures in addition to the static orientational disorder dictated by the placement of the pivotal oxygen atom on the fourfold c axis. For this reason the neutron data were taken at 8 K in the hope that the H scattering would be sufficiently localized to allow its detection. As in the x-ray study, we refined on the structure factors, F_o, using a weight $1/(\sigma')^2$ where $\sigma' = [\sigma^2 + (0.05F_o)^2]^{1/2}$. A small isotropic extinction correction of standard form was incorporated in the refinement.

Our initial refinement did not include the defect water molecule and yielded the discrepancy factors $R = 0.046$ and $R_w = 0.065$ for all hkl. From the outset the Br thermal parameters were ill behaved if of an anisotropic form and had to be refined isotropically in order to avoid a nonpositive definite form. Fourier difference maps clearly indicated the proton sites near O(1) and O(2) as well as the site II defect, O(3). However, the noise level in the map precluded an unambiguous assignment of the associated H sites near O(3). In order to rectify this problem, only the 353 reflections defined by $\Delta I/I <$ 0.10 were used in the map and an artificial overall Debye–Waller factor was employed to minimize the noise introduced by Fourier series truncation.

Figure 3 shows such a map where the negative peaks are interpreted as the hydrogens of the water molecule orientationally disordered about the fourfold c axis. Due to the rather small signal to noise ratio and

Table II. Coordinates[a] and Occupation Probabilities per Unit Cell for $K_2Pt(CN)_4Br_{0.30}\cdot 3.2H_2O$[b]

Atom	Equipoint and site symmetry	Occupation probability	x	y	z
Pt(1)	1a, 4mm	1	0	0	0
Pt(2)	1a, 4mm	1	0	0	0.4991 (2), 0.500 (1)
C(1)	4e, m	4, 4.00 (8)	0.2007 (7), 0.2033 (2)	0	0.0162 (23), 0.0051 (10)
C(2)	4d, m	4, 4.08 (9)	0.1430 (10), 0.1438 (3)	x	0.5151 (24), 0.4986 (9)
N(1)	4e, m	4, 3.91 (7)	0.3173 (8), 0.3212 (2)	0	0.0250 (19), 0.0132 (9)
N(2)	4d, m	4, 3.94 (7)	0.2252 (10), 0.2273 (3)	x	0.5069 (24), 0.4905 (9)
O(1)	4d, m	4, 3.60 (16)	0.3396 (12), 0.3392 (8)	x	0.9395 (21), 0.9338 (15)
O(2)	2c, mm	2, 1.88 (7)	1/2	0	0.6126 (24), 0.5974 (11)
O(3)	1b, 4mm	0.44 (3), 0.42 (4)	1/2	1/2	0.348 (9), 0.358 (7)
K(1)	4f, m	4, 3.80 (15)	0.1933 (2), 0.1945 (6)	1/2	0.2672 (15), 0.2581 (13)
Br(1)	1b, 4mm	0.608 (8), 0.592 (56)	1/2	1/2	0.4995 (18), 0.5127 (19)
H(1)	4d, m	3.36 (34)	0.279 (2)	x	0.848 (3)
H(2)	4d, m	3.76 (32)	0.372 (5)	x	0.815 (3)
H(3)	4e, m	3.92 (16)	0.4239 (8)	0	0.701 (2)
H(4)	4d, m	0.88 (32)	0.44 (3)	x	0.56 (3)

[a] Coordinates are of form x ray (296 K), neutron (8 K); for protons, neutron data only. Pt(1) was chosen as the origin for the noncentrosymmetric unit cell. Crystal data for KCP(Br): tetragonal system; Laue group *mmm*; space group No. 99, *P4mm*; x ray (296 K), $a = 9.890$ (7) Å, $c = 5.789$ (2) Å, $Z = 2$, $d_{calcd} = 2.47$ g/cm^3, $d_{obsd} = -$; (neutron, 8°K): $a = 9.829$ (4) Å, $c = 5.705$ (3) Å. [b] The least-squares estimates are enclosed in parentheses and are right adjusted.

the larger thermal motion associated with the H atoms, one cannot expect the ratio of the O and H peak heights to scale as the ratio of their respective scattering lengths, but the rough agreement exhibited in Figure 3 is encouraging. The ratio of the real O:H peak heights is not dependent on the choice of the artificial Debye–Waller factor while the ratio for artifacts, stray peaks and bands, in the map is noticeably reduced by its inclusion. As a check on the self-consistency of the H peaks we included the O(3) site in the refinement and repeated the difference map. The O(3) peak was reduced by a factor of 10 while the negative peaks remained unaltered.

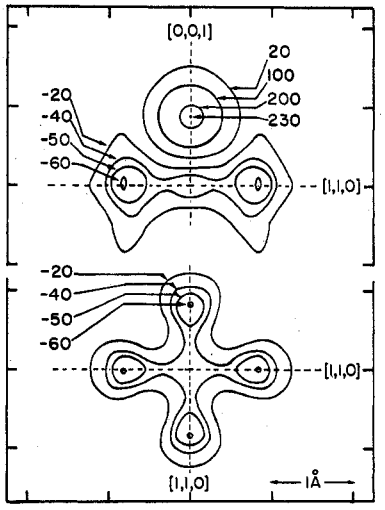

Figure 3. Neutron difference Fourier map of 8-K data. The top shows the section of the plane (x, x, z). The coordinate reference is at ($1/2$, $1/2$, 0.5), and the O site, at ($1/2$, $1/2$, 0.36). The bottom shows the section of the plane (x, y, 0.49). The coordinate reference is ($1/2$, $1/2$, 0.49). The contour values are proportional to the scattering length density. (Note the opposite sense of the z axis in this figure.)

Although difference maps are a powerful tool for indicating the existence and location of atomic sites not included in the initial refinement, their interpretation can be ambiguous for noncentrosymmetric structures exhibiting peaks near symmetry planes. In our case the maxima of the H peaks lie suspiciously close to the plane $z = 0.5$. If the defect water is "ideal", the H peaks would be displaced toward the O(3) site by an amount $\Delta z/3$ where Δz is the difference between the z coordinates of the two sites. How such a positional indetermination, pseudosymmetry, can occur is easily understood from the following argument.

Consider a one-dimensional structure with an atom located at $z = 0.5 + \delta$. The contribution of this atom to the complex structure factor, F, at the reciprocal lattice point $\bar{G}$ is $F(\bar{G}) = \exp(i\bar{G}\cdot\bar{Z}) = (-1)^l[\cos(2\pi l\delta) + i \sin(2\pi l\delta)]$. For small δ the low-frequency structure factors will "see" our test atom only through their real components. However, the real component cannot differentiate between the atomic site at δ and its ghost at $-\delta$. This differentiation is provided by the imaginary component which first becomes appreciable for δl of the order of $1/8$. If the atom has a large thermal motion, these components will be suppressed by the Debye–Waller factor and could be lost in the statistical error, especially if other noncentrosymmetric features of the structure contribute strongly to these reflections. Thus, a set of measured reflections containing few

Table III. Thermal Parameters[a] ($\times 10^4$) in Å^2 for KCP(Br)

Atom	U_{11}	U_{22}	U_{33}	U_{12}	U_{13}	U_{23}
Pt(1)	161 (3), 52 (9)	U_{11}	148 (3), 45 (12)	0	0	0
Pt(2)	178 (4), 50 (19)	U_{11}	157 (3), 44 (12)	0	0	0
C(1)	250 (26), 78 (12)	265 (26), 107 (12)	212 (40), 82 (11)	0	44 (38), =0	0
C(2)	256 (31), 88 (19)	U_{11}	262 (42), 113 (11)	6 (21), =0	−56 (61), =0	U_{13}
N(1)	276 (27), 65 (10)	482 (39), 175 (10)	331 (58), 104 (9)	0	65 (35), 35 (10)	0
N(2)	387 (41), 106 (14)	U_{11}	436 (44), 126 (10)	91 (28), −331 (58)	151 (70), =0	U_{13}
O(1)	736 (76), 257 (42)	U_{11}	727 (80), 266 (37)	33 (56), =0	−199 (86), −109 (32)	U_{13}
O(2)	441 (62), 46 (26)	866 (95), 262 (28)	369 (58), 75 (24)	0	0	0
O(3)	542 (332), 398 (245)	U_{11}	820 (388), 451 (256)	0	0	0
K(1)	421 (10), 152 (27)	448 (10), 107 (25)	569 (19), 113 (25)	0	8 (13), 57 (20)	0
Br(1)	281 (14), 25 (79)	U_{11}	443 (16), 25 (69)	0	0	0
H(1)	528 (112)	U_{11}	915 (135)	−721 (555)	−354 (121)	U_{13}
H(2)	1321 (302)	U_{11}	411 (74)	4691 (1491)	312 (174)	U_{13}
H(3)	213 (38)	493 (48)	335 (40)	=0	156 (31)	U_{13}
H(4)	2353 (3551)	U_{11}	1404 (1312)	0	0	0

[a] Values listed are of form x ray (296 K), neutron (8 K); neutron data only for H atoms. Some U_{ij} values, shown as "=0", refined to near-zero magnitudes with large esd's. These parameters were fixed during the final cycles of refinement. Parameters are from the thermal function of the form $\exp[-2\pi^2\Sigma_{i=1}^{3}\Sigma_{j\leq i}^{3}C_{ij}h_ih_ja_i^*a_j^*U_{ij}]$ where $C_{ij} = 1$ for $i = j$ and $C = 2$ otherwise. The estimates of error are enclosed in parentheses and are right adjusted.

Table IV. Some Atomic Distances (Å) and Angles (deg) for KCP(Br)[a]

1. $Pt(CN)_4$ Chain

Distances	X	N	Angles	X	N
Pt(1) → Pt(2)	2.889 (2)	2.848 (3)	C(1)-Pt(1)-C′(1)	174.6 (7)	178.3 (3)
Pt(2) → Pt(1)	2.900 (2)	2.844 (3)	C(2)-Pt(2)-C′(2)	174.7 (8)	179.7 (3)
Pt(1)-C(1)	2.007 (7)	2.001 (3)	Pt(1)-C(1)-N(1)	179.8 (9)	178.5 (4)
Pt(2)-C(2)	2.007 (7)	2.002 (3)	Pt(2)-C(2)-N(2)	175.0 (1.0)	177.9 (3)
C(1)-N(1)	1.169 (10)	1.164 (3)			
C(2)-N(2)	1.170 (10)	1.164 (3)			

2. K^+ Coordination Polyhedron

Distances	X	N	Angles	X	N
K(1)-N(1)	2.980 (6)	2.949 (5)	O(1)-K(1)-N(1)	71.2 (2)	71.5 (2)
-N(2)	3.068 (7)	3.008 (3)	-O′(1)	67.2 (3)	68.2 (2)
-O(1)	2.87 (1)	2.818 (7)	-N(1)	110.4 (3)	110.5 (2)
-O(2)	2.77 (1)	2.720 (7)	-O(2)	145.9 (1)	145.2 (1)
-O(3)	3.066 (8)	3.06 (1)	-N(2)	75.9 (2)	74.7 (1)
-Br(1)	3.318 (4)	3.336 (8)	-Br(1)	78.8 (2)	80.3 (3)
			-O(3)	66.5 (8)	68.1 (6)

3. Oxygen Atom Coordination

(a) Water Oxygen O(1)

Distances	X	N	Angles	N
O(1)-H(1)		1.03 (1)	H(1)-O(1)-H(2)	94 (2)
-H(2)		1.00 (3)	K(1)-O(1)-K′(1)	97.8 (3)
-K(1)	2.87 (1)	2.826 (9)	K(1)-O(1)-H(1)	111.4 (9)
-N(2)	2.97 (2)	2.977 (6)	K(1)-O(1)-H(2)	121.5 (1.2)
-C(2)	3.69 (1)	3.68 (1)		
-Br(1)	3.39 (1)	3.28 (1)	O(1)-H(2)-Br	168 (3)
-O(3)	4.10 (4)	3.97 (3)	-O(3)	180 (2)
-H(4)		2.6 (2)	O(1)-H(1)-N(2)	139 (1)
-C(2)	3.69 (1)	3.68 (1)	-C(2)	163 (1)

(b) Water Oxygen O(2)

Distances	X	N	Angles	N
O(2)-H(3)		1.02 (1)	H(3)-O(2)-H(3)	103 (1)
-N(1)	2.99 (1)	2.955 (5)	K(1)-O(2)-K′(1)	89.3 (3)
-C(1)	3.77 (1)	3.73 (1)	O(2)-H(3)-N(1)	157.8 (7)
			-C(1)	179.6 (6)

(c) Water Oxygen O(3)

Distance	N	Angles	N
O(3)-H(4)	1.5 (2)	H(4)-O(3)-H(4)	74 (15)
		K(1)-O(3)-K′(1)	158.5 (5)

[a] The esd's, in parentheses, are right adjusted.

significant high-frequency observations may be sufficiently sensitive to indicate the existence of an atomic site while containing little information concerning its precise location to either side of the nodal plane $z = 0.5$.

This indefiniteness in the coordinate also caused difficulty in the subsequent refinement of the defect H(4) parameters. Refinements starting from various initial conditions for the H(4) parameters and employing data sets of various significance levels confirmed the concentration of negative scattering on the (110) planes indicated in the difference map and yielded occupational probabilities consistent with the identification of this scattering with the hydrogens of the defect water molecule. However, the z coordinate refined to values on the opposite side of the $z = 0.5$ plane from what one would expect based on the geometry of a water molecule. Since this coordinate can be constrained to resemble a free water molecule with minimal change in the R factors, one is probably not justified in attaching any significance to the refined value for this coordinate.

Our placement of the water molecule can be reconciled with the room[11] and nitrogen[12] temperature neutron studies of Williams et al. on hydrated KCP(Br) if we interpret their extra Br^- site as the oxygen of the water molecule and invoke the plausible assumption that the thermal disorder of the H atoms at these elevated temperatures precludes their detection with neutrons. We cannot reconcile our results with the room-temperature neutron study on deuterated KCP(Br) of Heger et al.,[14] who, on the basis of a difference map of unabsorption corrected data, oriented the water molecule with the H sites diametrically opposite from ours.

The final neutron structure refinement employed 83 parameters and 440 reflections and yielded the discrepancy factors $R = 0.039$ and $R_w = 0.056$ for all hkl with a goodness-of-fit index of 1.07. As a check on the stability of the refinement, all 83 parameters were varied simultaneously to convergence using a small stepping increment to prevent oscillatory behavior of some of the defect parameters. The resulting parameters are listed in Tables II and III; bond lengths, in Table IV. We fixed the occupation of the Pt sites at unity so that any error in the Pt scattering length will show up in the occupation numbers of the other atomic sites. This, along with some obvious water loss, may explain the tendency of most of the occupation number to be slightly less than ideal.

A few words seem in order on the validity of a standard structure refinement which ignores the intensities of the CDW satellite reflections. Since the sinusoidal lattice displacement can be regarded as a static phonon, one would expect the errors incurred by ignoring the superlattice reflections to show up in the thermal parameters of the displacing $Pt(CN)_4^{1.7-}$ groups. A discussion of this point is given in ref 9 where it is argued that for KCP(Br) the traditional thermal parameters will not be significantly altered by the inclusion of the CDW response.

Thermal Gravimetric Analysis. Supportive evidence for the defect water molecule was obtained from thermal gravimetric analysis (tga) of freshly grown deuterated crystals. The crystals were picked from solution, blotted dry, and immediately placed in a Du Pont 900

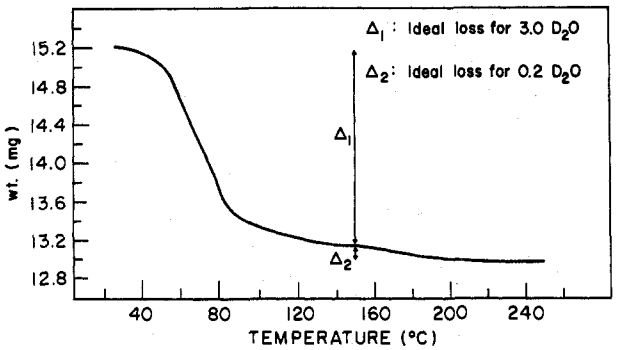

Figure 4. Thermal gravimetric analysis of deuterated KCP(Br) using heating rate of 3 °C/min.

differential thermal analyzer where they were heated to 250 °C at a rate of 3 °C/min. A representative result, shown in Figure 4, clearly indicates a two-step weight loss. A parallel mass spectrometric analysis identified these thermal decomposition products as water with no evidence for any Br^--containing species. The large step, occurring in the range 30–110 °C, corresponds to the 3 D_2O groups per formula unit which occupy the O(1) and O(2) sites in the unit cell. The small, but significant, step in the range 150–180 °C corresponds to the 0.2 D_2O which occupies the defect site.

Similar two-step tga curves were obtained using protonated KCP(Br) crystals which had been stored in a humidor for some weeks; however the total weight loss was always on the low side indicating some dehydration. The only available crystals still in solution happened to be deuterated. An earlier study concluded that $KCP(X)\cdot nH_2O$ formed a series of hydrates with $n = 2.5$–3.0.[18]

Partially dehydrated deuterio KCP(Br) crystals may not necessarily retain the defect water near the body center of the unit cell. Out of curiosity, crystals of deuterio KCP(Br) were dried under ambient conditions for 24 h and then subjected to tga. All the remaining water, ~0.5 D_2O, was released in one smooth step upon heating to only 90 °C.

IV. Discussion

The polar noncentrosymmetric structure is shown in Figure 1a and b and some of the interatomic distances are listed in Table IV. The structure is characterized by nearly planar, square $Pt(CN)_4^{1.7-}$ groups arranged in linear, polymeric chains parallel to the c axis with the two slightly different Pt–Pt distances per unit cell of 2.900 (2) and 2.889 (2) Å at 300 K. (In this section all distances and angles refer to the x-ray determination.) Each $Pt(CN)_4^{1.7-}$ unit is rotated 45° with respect to its nearest neighbors resulting in an arrangement of cubic antiprismatic, face-sharing polyhedra. These chains are supported and screened by a loosely bound cubic antiprismatic structure of K^+, Br^-, and H_2O molecules. The true stoichiometry for KCP(Br), as determined from our results, is $K_2Pt(CN)_4Br_{0.30}\cdot 3.2H_2O$.

Our structure is normal in terms of the waters of hydration in that an x-ray refinement on the occupation numbers of the oxygen sites O(1) and O(2), as well as the K^+ ion site, yielded unit occupations within experimental error. These two waters form part of the coordination sphere of the potassium ions comprised of four nitrogens, three oxygens, and either the Br^- ion or the oxygen of the defect water molecule.

The space-filling role of the defect water molecule is obvious from viewing the average structure in the (110) plane, Figure 5. This view supports our static orientation of the defect water at 8 K since the same volume of the unit cell is occupied by both kinds of defects. This would not be the case if the water had the orientation proposed by Heger, et al.[15] The dipole–dipole repulsion between the defect water molecule and the four water molecules on (110) planes is responsible for the large apparent thermal motion at 8 K exhibited by the protons H(1) and H(2). The O(1) positions are relatively more localized because of their coordination to a pair of K^+ ions in a neighboring cell via the sp^3 lone-pair electrons. In addition, the O(1) atom is always hydrogen bonded to a CN^- ligand at $z = 0.5$. The resulting motional response of this water molecule to the Br^- or water defects is constrained to a "rocking" in the (110) plane.

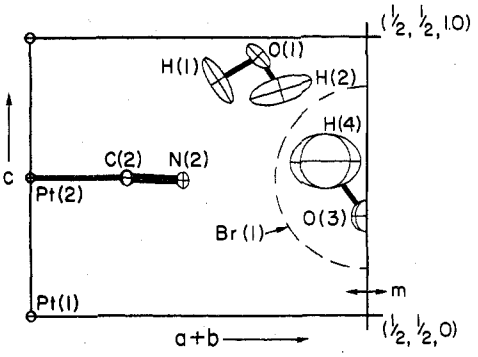

Figure 5. KCP(Br) structure in the (110) plane showing space-filling role of the defect water in the absence of the Br^- ion, dashed circle. Remainder of atoms shown using 50% probability ellipsoids.

The defect water molecule is axially disordered because the environment at the center of the cell does not permit strong hydrogen bonding or strong coordination of the oxygen, O(3), with the K^+ ions. In particular, the oxygens of the two normal waters, O(1) and O(2), are 2.87 (1) and 2.77 (1) Å from K^+ ions with K–O–K bond angles of 97.8 (3) and 87.4 (4)°, respectively. The defect oxygen is 3.07 (1) Å from a K^+ ion and has a K–O–K angle of 163 (2)° with the sp^3 orbitals pointing between two K^+ ions. The O(1)–N(2) distance of 2.97 (2) Å and the O(2)–N(1) distance of 2.99 (1) Å are significantly shorter than the O(3)–N(2) distance of 3.95 (1) Å indicating a much weaker CN--H–O interaction for the defect water than for the two normal waters. These CN--H–O interactions are strong enough to orient the $2/m$ water molecule in one of the two degenerate (110) planes at low temperatures. Although rotational motion of the defect water is easily excited, it is more difficult to displace thermally than the other two waters possibly because of its location where, on the average, twice as many interactions with the environment are possible.

The mixed-valence Pt oxidation state in KCP(Br) is accommodated by the polarizability of the CN^- ligands via the back-bonding of the π^* orbitals of CN^- with the d orbitals of Pt.[21] In fact, the presence of the Br ion is used to explain the partial oxidation of the Pt d_{z^2} band and the consequent metallic conductivity. Since the Br^- ion is far removed from a Pt atom, residing in the second-order coordination sphere, this polarization effect must be rather important. The incorporation of the defect water into a similar site as the Br^- ion can be attributed to a trans polarization of the CN^- groups by the Br^- ion. That is, the existence of a Br^- ion in one cell polarizes the CN^- groups, via the linear group $Br^-—N^+{=}C^-—Pt—C^+{=}N^-$, in the adjacent cells along the [110] directions and favors the occupancy of the center of these cells by the positive charge of the dipolar water molecule.

The $K^+\cdots CN^-$ attraction causes a pronounced nonplanarity in both $Pt(CN)^{1.7-}$ groups. In addition the $Br^-\cdots CN^-$ repulsion introduces a nonlinearity in the Pt—C≡N group at $z = 0.499$ (see Table IV and Figure 1b).

There are no obvious structural indications for the assignment of the II and IV oxidation states for the Pt atoms based on the first coordination sphere. Based on the second sphere coordination, the Pt at (0, 0, 0.499) is more electropositive than the Pt at the origin of the unit cell. In this sense, KCP(Br) is a mixed crystal in that the structure can be regarded as a random distribution of the two unit cells $K_4XY\cdot 6H_2O$ where X always represents $[Pt^{II}(CN)_4]^{2-}$ and

Y represents $[Pt^{III}(CN)_4Br]^{2-}$ in 60% of the unit cells and $[Pt^{II}(CN)_4H_2O]^{2-}$ in the remainder of the cells.

This formulation implies a Pt III oxidation state for some of the Pt sites at $z = 0.499$ while the random polymeric mixture of two kinds of sites results in an inability to recognize its distinct presence in the structure. Considering the lack of an octahedrally coordinated Pt(IV) polyion in KCP(Br), although both octahedral $K_2Pt(CN)_4Br_2$ and square-planar $K_2Pt(CN)_4$ are used to synthesize KCP(Br), an extremely reactive $[Pt^{III}(CN)_4Br]^{2-}$ square-pyramidal ion is a possibility during crystallization. In fact, Pt(III) complexes have been invoked to explain the kinetics of redox reactions between Pt(II) and Pt(IV).[22,23] Such an ion would most logically sit down on the *ab* face of a growing crystal of KCP(Br), and this happens to be the most active face with long, needle-shaped crystals resulting. As Br^- ions are accommodated into interstices of the growing crystals, the second Br^- of the Pt(III) complex is ionized into solution to maintain electrical neutrality. A recent EPR study of Magnus' green salt, $Pt(NH_3)_4PtCl_4$, was interpreted in terms of an electronic model formally equivalent to a substitution of Pt(III) for some of the Pt(II) sites due to the presence of Pt(IV) impurities during crystallization.[24]

Acknowledgment. We wish to thank M. Paputa for the TGA experiment, R. Saillant, R. Jaklevic, and S. Werner for valuable discussions, and B. Novak for computational assistance. The x-ray data were taken on a Syntex diffractometer kindly loaned to us by M. Glick and Wayne State University. The neutron data were taken at the Ford Nuclear Reactor at the University of Michigan.

Registry No. $K_2Pt(CN)_4 \cdot 3.2H_2O$, 14323-36-5; Br_2, 7726-95-6.

Supplementary Material Available: Tables V and VI, listing structure factor amplitudes for KCP(Br) (x-ray data at 300 K; neutron data at 8 K) (9 pages). Ordering information is given on any current masthead page.

References and Notes

(1) R. Comès, M. Lambert, H. Launois, and H. R. Zeller, *Phys. Rev. B*, **8**, 571 (1973).
(2) In ref 12 and 13 the term superstructure is unfortunately used in reference to the odd *l* reflections of the present structure.
(3) R. Comès, M. Lambert, and H. R. Zeller, *Phys. Status Solidi B*, **58**, 587 (1973).
(4) B. Renker, L. Pintschovious, W. Glaser, H. Reitschel, R. Comès, L. Liebert, and W. Drexel, *Phys. Rev. Lett.*, **32**, 826 (1974).
(5) K. Krogmann and D. Hausen, *Z. Anorg. Allg. Chem.*, **358**, 67 (1968).
(6) R. E. Peierls, "Quantum Theory of Solids," Clarendon Press, Oxford, 1955, p 108.
(7) A. W. Overhauser, *Phys. Rev. B*, **3**, 3173 (1971); *Phys. Rev.*, **167**, 691 (1968).
(8) J. W. Lynn, M. Iyumi, G. Shirane, S. A. Werner, and R. B. Saillant, *Phys. Rev. B*, **12**, 1154 (1975).
(9) C. F. Eagen, S. A. Werner, and R. B. Saillant, *Phys. Rev. B*, **12**, 2036 (1975).
(10) C. Peters and C. F. Eagen, *Phys. Rev. Lett.*, **34**, 1132 (1975).
(11) J. M. Williams, J. L. Peterson, H. M. Gerdes, and S. W. Peterson, *Phys. Rev. Lett.*, **33**, 1079 (1974).
(12) J. M. Williams, F. K. Ross, M. Iwata, J. L. Peterson, S. W. Peterson, S. C. Lin, and K. Keefer, *Solid State Commun.*, **17**, 45 (1975).
(13) H. J. Deiseroth and H. Schulz, *Phys. Rev. Lett.*, **33**, 963 (1974).
(14) H. J. Deiseroth and H. Schulz, *Mater. Res. Bull.*, **10**, 225 (1975).
(15) G. Heger, B. Renker, H. J. Deiseroth, H. Schulz, and G. Scheiber, *Mater. Res. Bull.*, **10**, 217 (1975).
(16) R. B. Saillant, R. C. Jaklevic, and C. D. Bedford, *Mater. Res. Bull.*, **9**, 289 (1974).
(17) Modified versions of the following programs for a PDP-10 computer were used in our work: (a) W. Schmonsee's program for the correction of diffractometric data and estimation of statistical errors, (b) B. Weunsch's absorption correction program, (c) FORDAP, A. Zalkin's Fourier summation program, (d) ORFLS and ORFEE, W. Busing, K. Martin, and H. Levy's least-squares and function and error programs, and (e) ORTEP, C. K. Johnson's crystal drawing program.
(18) D. Cahen, *Solid State Commun.*, **12**, 1091 (1973).
(19) "International Tables for Crystallography", Vol. III, Kynoch Press, Birmingham, England, 1962, p 201.
(20) R. B. Saillant and R. C. Jaklevic, *ACS Symp. Ser.*, **No. 5**, 376 (1974).
(21) F. Basolo and R. G. Pearson, "Mechanisms of Inorganic Reactions", Wiley, New York, N.Y., 1967, p 367.
(22) R. L. Eich and H. Taube, *J. Am. Chem. Soc.*, **76**, 2608 (1954).
(23) G. E. Adams, R. B. Broskiewicz, and B. D. Michael, *Trans. Faraday Soc.*, **64**, 1256 (1968).
(24) B. A. Scott, R. Mehran, B. D. Silverman, and M. A. Ratner, *ACS Symp. Ser.*, **No. 5**, 331 (1974).

Contribution from the Departments of Chemistry, State University of New York at Buffalo, Buffalo, New York 14214, and the University of Illinois at Chicago Circle, Chicago, Illinois 60680

Transition Metal σ-Acyls and Related Species. IV.[1-3] Crystal Structure and Molecular Geometry of $MeCH{=}CH{=}CHCHMeOC(=O)Fe(CO)_3$, a Molecule Containing an Fe—C(Carboxylate) Linkage in a Ferrelactone Ring

MELVYN ROWEN CHURCHILL* and KAN-NAN CHEN

Received September 3, 1975 AIC50653I

The stereochemistry of the species $MeCH{=}CH{=}CHCHMeOC(=O)Fe(CO)_3$, prepared by Moriarty et al. from the reaction of iron carbonyl with the monoepoxide of *cis,trans*-hexa-2,4-diene, has been determined unambiguously by means of a single-crystal x-ray diffraction study. The complex crystallizes in the centrosymmetric orthorhombic space group *Pbca* [D_{2h}^{15}; No. 61] with $a = 12.0732$ (16) Å, $b = 15.2272$ (12) Å, $c = 12.2010$ (15) Å, $V = 2243.04$ Å^3, and $Z = 8$. X-ray diffraction data complete to $2\theta = 50°$ (Mo Kα radiation) were collected with a Picker FACS-1 automated diffractometer, and the structure was solved by conventional Patterson, Fourier, and least-squares refinement techniques. All atoms (including hydrogens) were successfully located, the final discrepancy indices being $R_F = 3.21\%$ and $R_{wF} = 3.06\%$ for the 1434 independent reflections (none rejected). The molecule has the skeletal form $MeCH{=}CH{=}CH{-}CHMeOC(=O)Fe(CO)_3$ and contains a ferrelactone ring. The iron atom is bonded to three carbonyl ligands (Fe–CO = 1.784 (3), 1.798 (3), and 1.826 (3) Å), to a π-allylic fragment (Fe–C(3) = 2.090 (2), Fe–C(4) = 2.077 (3), Fe–C(5) = 2.209 (3) Å), and to a lactone system, the Fe–C σ-bond distance in the FeC(=O)OR system being 1.985 (2) Å.

Introduction

The vinylcyclopropyl system is known to react with iron carbonyl to yield a species which contains both a (π-allyl)→iron and a (σ-acyl)→iron linkage;[4] see eq 1.

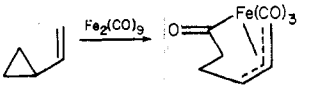

(1)

Vinyl epoxides (vinyloxiranes) react analogously, resulting in species containing a (π-allyl)→iron linkage and an Fe–C (iron–carboxylate) σ linkage;[5] see eq 2.

* To whom correspondence should be addressed at the State University of New York at Buffalo.